Available online at www.sciencedirect.com
ScienceDirect
Applied Surface Science 254 (2007) 1073–1078
applied surface science
www.elsevier.com/locate/apsusc

Laser processing of micro-optical components in quartz

G. Kopitkovas [a,b,c,*], T. Lippert [a], N. Murazawa [b], C. David [a], A. Wokaun [a], J. Gobrecht [a], R. Winfield [c]

[a] Paul Scherrer Institut, CH-5232, Villigen PSI, Switzerland
[b] Building, Sapporo 001-0021, Japan
[c] Tyndall National Institute, Lee Maltings, Prospect Row, Cork, Ireland

Available online 22 September 2007

Abstract

Laser induced backside wet etching combined with the diffractive gray tone phase mask has been used for the fabrication of a micro-lens array with a single lens diameter of 1 mm and a micro-prism in quartz. The micro-lens array was tested as beam homogenizer for high power XeCl excimer laser yielding a clear improvement in the quality of the laser beam.

The optimum fluence range for fabrication of micro-lenses by laser induced backside wet etching using 1.4 M pyrene in THF solution and 308 nm irradiation wavelength is 1–1.6 J/cm^2. The etching mechanisms of LIBWE are based on a combination of pressure and temperature jumps at quartz–liquid interface.

Keywords: LIBWE; Micro-optics; Beam homogenizer; Quartz

1. Introduction

Quartz is a material that exhibits a chemical and mechanical stability and large optical transparency over a wide wavelength range (200–2000 nm). These properties make quartz the key material for many fields, such as optical communication, high quality imaging system, beam wave front measurements, multiple beam shaping and homogenizing [1]. Many of these applications require three-dimensional optical components, i.e., waveguides, micro-lenses, micro-prisms, or micro-mirrors. The technology, which is used for the fabrication of optical elements in UV transparent materials, is a combination of lithography and reactive ion etching (RIE) [1–4]. This technology with relatively high throughput has also some drawbacks. First of all, several techniques (e.g., lithography, resist reflow and RIE) must be combined and the technology is also sensitive to the materials properties, which are etched, e.g., in proportional to etching of the photopolymer and quartz. Furthermore, etching of other UV transparent, e.g., BaF_2, CaF_2 or sapphire, by RIE is very difficult due to the material properties. Furthermore, many steps are required in this process, which must all be well controlled. An alternative technique for direct structuring of quartz is laser writing, where deep ultraviolet (DUV) or ultrafast (fs) lasers are applied [5–9]. This approach can be used to fabricate two-dimensional diffractive optical elements [10] or three-dimensional structures inside the quartz [11]. These lasers are not used so far for the generation of three-dimensional components in the quartz surface, although the etch roughness of quartz structured by fs or DUV lasers is low ($\leq$100 nm). An alternative technology, which seems to be attractive for the fabrication of three-dimensional structures in quartz and other UV transparent materials is an indirect laser assisted etching process. The laser light passes through the transparent material, which is in contact with strongly absorbing media, which can be in the form of, e.g., pyrene in different solvents (acetone, tetrahydrofurane (THF), cyclohexane, tetracyclohexane and toluene) [12–25], aqueous pyranine or naphthalene [26,27], pure toluene [18,21,28–31] and naphthalene in methyl-methacrylate [32,33]. The etching of UV transparent materials, e.g., polytetrafluorethylene (PTFE), quartz, CaF_2, BaF_2 and sapphire) [12–27,29–40] by laser induced backside wet etching

* Corresponding author. Present address: ABB Switzerland Ltd, Fabrikstrasse 3, CH-5600, Lenzburg, Switzerland. Tel.: +41 79 2646074; fax: +41 58 5861308.
E-mail address: giedrius.kopitkovas@ch.abb.com (G. Kopitkovas).

0169-4332/$ – see front matter
doi:10.1016/j.apsusc.2007.09.048

(LIBWE) using various lasers occurs due to the high temperature and pressure jump which is created at the material–liquid interface. This approach is applied to create microfluidic devices [22,41] and high resolution optical gratings with a period down to 105 nm [17,34,35]. The combination of LIBWE with a projection of a diffractive gray tone phase mask (DGTPM) opens a new way for fast and simple fabrication of diffractive (Fresnel) and refractive (plano-convex) micro-lens arrays [23,38,40] or even more complex structures such as pyramids.

In this manuscript we focus on the application of XeCl excimer radiation (308 nm) and 1.4 M pyrene in THF solution. This laser and solution are selected because of the wide fluence range in which the lowest etch roughness is obtained. This fluence range is also applied for the fabrication of micro-optical elements in quartz.

The mechanism of LIBWE and the application of this method for the application of micro-lenses in quartz are discussed in this paper. The idea of laser light modulation by DGTPM and its projection at the quartz–liquid interface, where also an etching occurs, is also described in this manuscript. Finally, it will be shown, that the micro-lenses, fabricated by LIBWE, can be applied as beam homogenizers for improving the XeCl excimer laser beam.

2. Experimental

Three-dimensional structures in quartz are fabricated by the LIBWE technique and the experimental system for the projection of a DGTPM on the surface to be patterned is shown in Fig. 1.

1.4 M pyrene in tetrahydrofurane solution was applied as etching media. The XeCl excimer laser beam (308 nm, 30 ns (FWHM)) passes through an attenuator plate which controls the intensity of the laser light, followed by a round shape mask and the DGTPM which modulates the incoming laser beam intensity into a beam with the desired radial energy distribution [42]. This modulated beam is imaged onto the quartz–liquid interface, where the etching of quartz occurs. The imaging of the beam is achieved by using an air spaced lens with a focal length of 100 mm and a diameter of 25 mm. The distance between the mask and lens, and between the lens and target is set according to the Eqs. (1) and (2):

$$a = f(M+1), \tag{1}$$

$$b = \frac{f(M+1)}{M}. \tag{2}$$

where a is the distance between the DGTPM and the lens, b is the distance between the lens and the quartz plate, f is the focal length of the lens, and M is the demagnification (a five times demagnification is used in our experiment). The diameter of the DGTPM is 5 mm. The round shape mask is placed at a distance of 1 mm behind the DGTPM and is adjusted that the image of the DGTPM fits exactly within the mask. The distance a was set to 600 mm, while the distance b was carefully set to 120 mm in order to get the highest resolution of the DGTPM image in quartz. The diameter of the resulting single refractive lens was 1 mm. The arrays, which consist, e.g., of 10 × 10 lenses were fabricated by a step and repeat technique.

3. Results and discussion

Prior to describing the fabrication and testing of micro-optical elements, it is noteworthy to consider the LIBWE process and possible etching mechanism.

LIBWE is a process, where etching of UV transparent materials is induced most probably by the creation of high temperature and pressure shocks at the very thin material–liquid layer. The light of the UV laser passes through the UV transparent material, and is strongly absorbed by the liquid, which is in contact with the material. The liquid can be, for example, a solution of pyrene molecule, which is electronically excited by the laser light. The non-radiative relaxation of the excited molecules results in the generation of a high temperature jump. The temperature can reach ≥2000 °C within the laser pulse [13,33]. This temperature jump causes heating, melting or even boiling of the material surface, which is in contact with the solution. The rapid increase in the temperature at the quartz–liquid interface during the laser pulse generates high pressure shock waves during an explosive boiling of the solution, which travel toward the quartz and solution [29,31,33,43]. The value of this pressure jump can reach 70 MPa (700 bars) [29,31,33]. This pressure is strong enough to remove *molten* material from the surface. The pressure jump drops down within the couple of microseconds after the laser pulse due the expansion of the shock wave in the solution, which travels with the speed of sound through solution. The temperature decreases rapidly due to the efficient cooling process by the solution [33]. After rapid decay in the

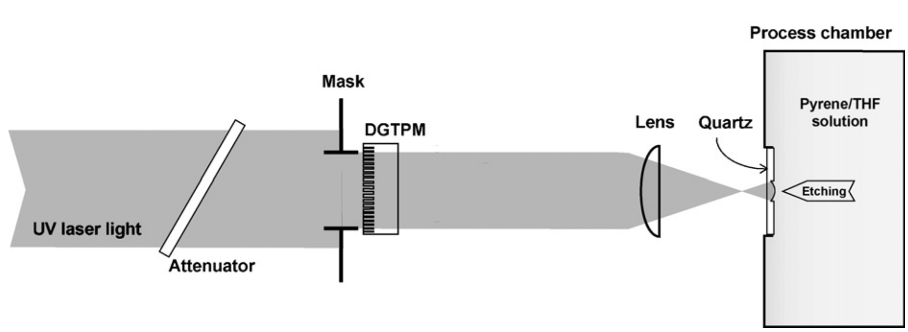

Fig. 1. Experimental setup for the fabrication of quartz micro-lenses by LIBWE and DGTPM.

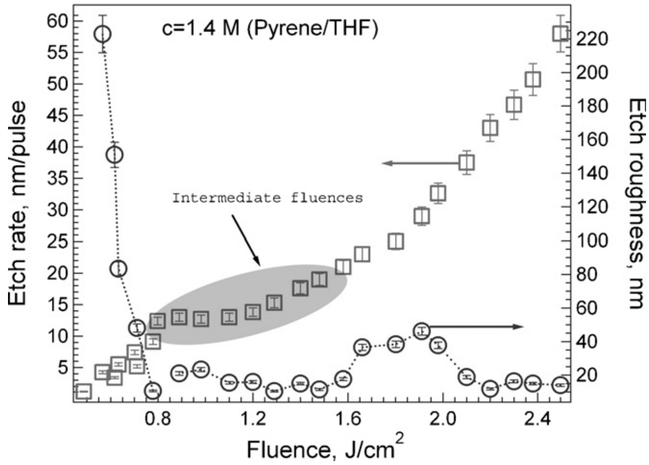

Fig. 2. The etch rate and the etch roughness as functions of the laser fluence at 308 nm by LIBWE using 1.4 M pyrene in THF solution.

temperature and pressure jumps the bubble is formed at the quartz–liquid interface. This bubble grows to its maximum radius followed be the shrinkage and collapse [28,33]. The latter process generates a second pressure jump, which is directed towards the quartz surface. This pressure increase, however, most probably does not influence the LIBWE process, because the time necessary for the formation of the bubble, its growth and collapse, is longer than 200 μs. The temperature at the quartz–liquid interface at this time is, according to Vass et al. [33], well below the melting point of quartz.

The basis for the fabrication of micro-optical elements is the determination of the etch rate and roughness as fraction of the process parameters such solution, pyrene concentration and laser fluence. The knowledge of this data is necessary to fabricate the micro-optical elements with the best possible surface quality.

The etch rates of quartz by LIBWE and 1.4 M pyrene in THF solution are shown in Fig. 2. The lowest laser fluence for which etching can be observed with the 1.4 M pyrene in THF solution is 0.48 J/cm^2 for 308 nm irradiation. The etched areas at these low fluences are coated with black carbon deposits that have been also observed for a 0.4 M pyrene in acetone solution at the low fluence range [23,40] and also for other solutions and laser wavelengths [19]. The laser induced temperature increase at these fluences does probably not reach the melting point of quartz. The structuring occurs, however, after a number of laser pulses (incubation pulses) [16,23] during which a carbon film is formed [19,23]. This film increases the absorption of the laser light in the layer resulting in a higher temperature increase, which may now melt the quartz. The etch roughness at these fluences are relatively high, as shown in Fig. 2, and a carbon layer exists in the etched areas, which makes these laser fluences unfavorable for the creation of micro-optical elements.

The etching mechanism at the fluences between 0.8 and 1.7 J/cm^2 (which is also marked as ‘‘intermediate fluences’’ in Fig. 2) is, as described above, dominated by melting of the material surface and a smooth removing by the pressure waves. Optically smooth etch areas are obtained at this fluence range. The roughness is in the range of 5–30 nm, and almost no carbon deposits are determined. *These fluences are the most favorable for the fabrication of the micro-optical elements in quartz.*

The temperatures at fluences above 1.8 J/cm^2 are high enough to create a plasma in the solution [40]. The generation of the plasma results probably in increase of the pressure jump. Interaction of the plasma with quartz results in an increase in the etch rates, but also in increase in the etch roughness which makes this fluence range again unfavorable for our applications.

The fabrication of micro-optics in quartz is performed, as discussed above, by a combination of LIBWE with the projection of a DGTPM. The DGTPM consist of periodical line structures with a various width. A typical DGTPM consists of 1000–3000 lines etched in quartz by using e-beam lithography and RIE. The zero order transmission of the light through this type of mask depends on the line width, line depth, and spacing between the lines (grating pitch) and can be described by Eq. (3) [42]:

$$\frac{F}{F_0} = \frac{p^2 - 2w(p-w)}{p^2}\left[1 - \cos\left(\frac{h \times 2(n-1)\pi}{\lambda}\right)\right], \tag{3}$$

where F is the laser fluence transmitted in the 0th order of the grating, F_0 is the incoming laser fluence, p (=5 μm) is the grating pitch, h (=180 nm) is the depth of the structures, w is the width of the lines, n (=1.5) is the index of refraction for quartz at 308 nm and λ (=308 nm) is the laser wavelength.

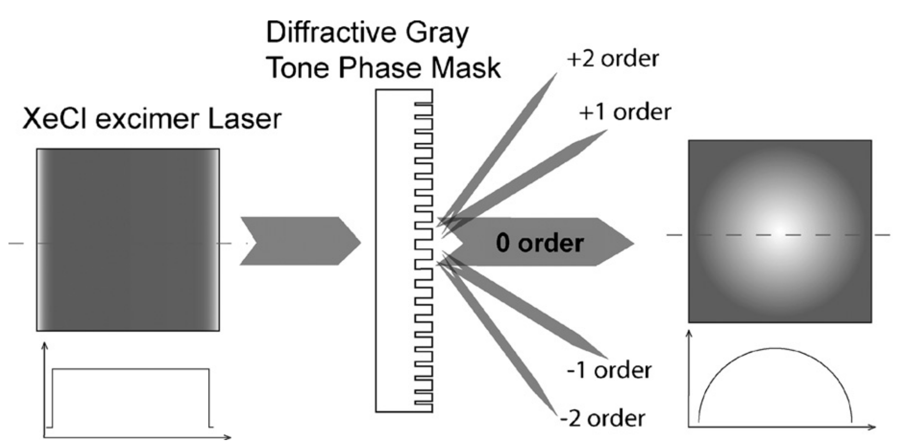

Fig. 3. Scheme of the modulation of an incoming laser beam using a DGTPM.

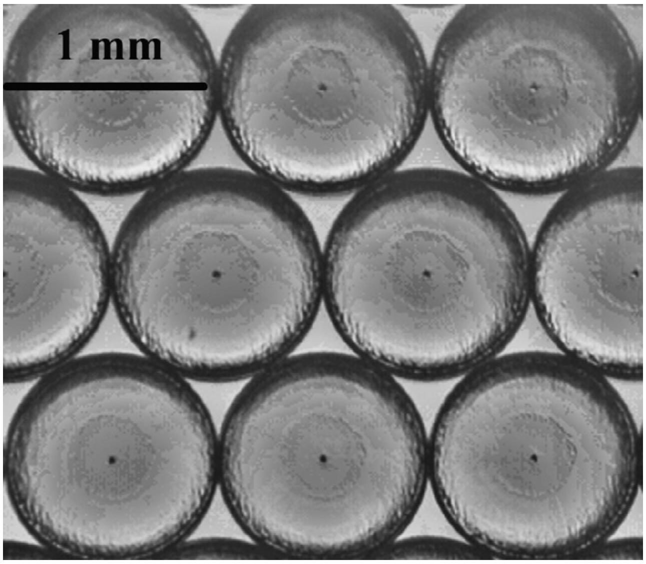

Fig. 4. Area of a micro-lens array fabricated in quartz by LIBWE.

The depth of the structures is chosen in a way, that the minimum fluence, which is transmitted through the grating, is $F = 1\ \mathrm{J/cm^2}$, for an incoming laser fluence $F_0 = 1.6\ \mathrm{J/cm^2}$. The line width for this minimum is $w = 2.5\ \mu\mathrm{m}$. The fluence, transmitted through the grating, increases continuously with the decrease of the line width. The maximum fluence, which is transmitted by this grating in the 0th order, is $1.6\ \mathrm{J/cm^2}$. The grating is therefore designed to utilize only the fluences from the ''intermediate'' fluence range, where the lowest etch roughness is obtained. The structures of the DGTPM with various line widths allow us also to modulate the incoming light into spherical shape symmetry, as illustrated in Fig. 3. The laser intensity, which is modulated by the mask, is imaged on the backside of the quartz, where the etching occurs. An array of, e.g., 10×10 micro-lenses in quartz (shown in Fig. 4) can be fabricated by a step and repeat process. Each lens has a diameter of 1 mm with a focal length of 60 mm and is fabricated by using 200 laser pulses with a repetition rate of 9 Hz, yielding a total fabrication time of the lens array of 40 min. The machining time is limited by our laser system, but not by the method itself. The application of high repetition lasers extends LIBWE method and may drastically shorten the machining time, as was already demonstrated by Niino et al. [44]. The micro-lens array can be applied as beam homogenizers, for e.g., the XeCl excimer laser beam. The concept of beam homogenizing with a micro-lens array is based on the splitting of the laser beam into many beamlets, which are directed onto the target by a single lens. The intensity of each beamlet is distributed over the complete area at the focal plane of

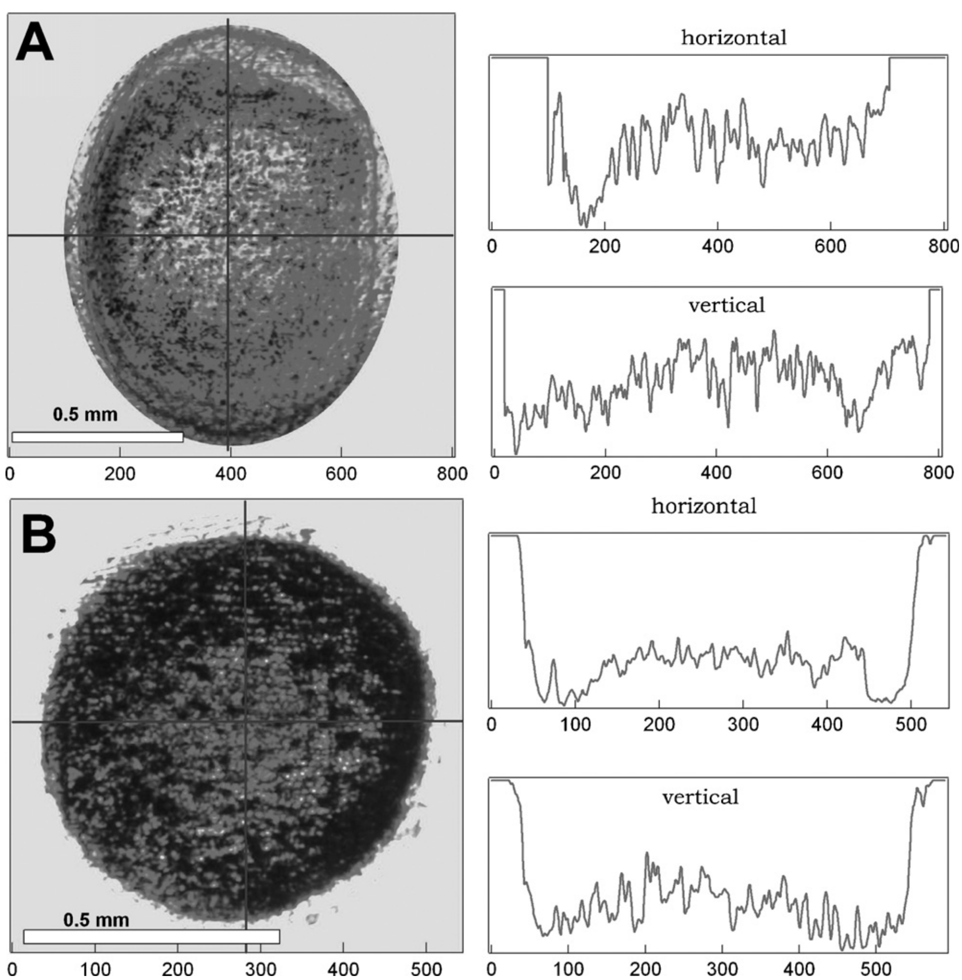

Fig. 5. XeCl excimer laser beam profile transferred by ablation into polyimide (A) with and (B) without the beam homogenizer with the corresponding line scans.

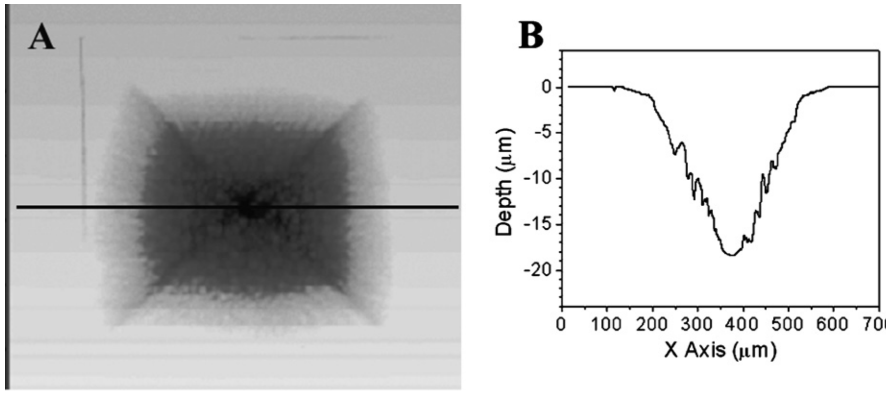

Fig. 6. Image of micro-prism etched in quartz by (A) LIBWE and (B) the corresponding line scan.

the collecting (field) lens resulting in an equivalent energy distribution over the area [45]. An incoming laser beam with an uneven intensity distribution is therefore converted into a beam with a homogenous energy distribution. At the first thought it appears that an increase of number of micro-lenses in the array should result in a better homogenizing of the beam. A high number of micro-lenses can be achieved most easily by reducing the diameter of the lenses. This approach has, however, a serious drawback: an increase in the number of micro-lenses with smaller diameter results in creation of periodically spaced patterns in the homogenized laser beam profile. This is due to the splitting of the incoming beam with a relative high degree of coherence into many beamlets. The beamlets, which are slightly different in phase due to imperfections of the micro-lenses and diffraction through the micro-lens pupil, will interfere with each other at their superposition plane, which is the focal plane of the collecting lens (and also coincidences with the homogenizing plane) [38,46]. The period of these patterns will decrease with an increase of the micro-lenses diameter. We fabricated therefore a homogenizer with an array of micro-lenses with a diameter of each lens of 1 mm.

The beam homogenizer based on the micro-lens array fabricated by LIBWE consists of a single micro-lens array and a collecting lens was tested for improving the quality of excimer lasers beams. The inhomogeneous part of the XeCl excimer laser beam is selected with the mask in order to test our beam homogenizer. The beam profile of the XeCl excimer laser with and without homogenizer is transferred into polyimide by ablation (shown in Fig. 5). This approach has been chosen because the ablation quality and structures are closely related and are very sensitive to the energy distribution of the beam. The homogenized XeCl excimer laser beam profile reveals a more homogenous intensity distribution and has a round shape (shown in Fig. 5B) compared to the structures obtained without homogenizer (shown in Fig. 5A). The beam homogenizer creates not only the homogeneous energy distribution at the focal plane of the collecting lens but also round shape of the beam. This shows that LIBWE and the projection of DGTPM can be used for the fabrication of high quality micro-lens arrays, which can be applied as beam homogenizers for high power lasers. Even better results of homogenization have been obtained (not shown) when two lens arrays have been applied.

The combination of DGTPM's with LIBWE opens additionally a new exciting way to fabricate complex three-dimensional structures, such as micro-prisms in quartz, which are difficult to fabricate with other techniques, e.g., with melt-reflow. The first example of such structures in quartz and a corresponding line scan is shown in Fig. 6.

The design for this structure has not yet been optimized, which is the origin for the high etch roughness of the structure. Anyhow, this is the first example of the potential of this technique in the fabrication of structures with complex geometries, e.g., lenses, prisms, etc., which are very difficult to create by other techniques.

4. Conclusion

Laser induced backside wet etching is a *one-step* etching process for UV transparent materials, with three different fluence dependent etching mechanisms. The mechanism at the low laser fluences is based on the combination of carbon formation and shock wave pressure, resulting in a high etch roughness. Surface melting and a pressure jump are important for the etching process at intermediate laser fluences, which yields the lowest etch roughness. Boiling of material surface, plasma formation in solution and high pressure waves are the origins for material remove with higher etch roughness at high laser fluences. The fabrication of three-dimensional optical components (micro-lens arrays and micro-prism) is achieved by the combination of LIBWE with projection of the DGTPM using the intermediate fluence range. The simple combination of micro-lens arrays with a single lens can be applied as beam homogenizer for the XeCl excimer laser.

Acknowledgment

The authors are grateful Dr. Konstantins Jafimovs for the fabrication of DGTPM for pyramid shape structures.

References

[1] S. Sinzinger, J. Jahns, Microoptics, Wiley-VCH GmbH & Co. KGaA, Weinheim, Germany, 2003.

[2] H.P. Herzig, Micro-optics Elements Systems and Applications, Taylor & Francis Ltd, London, 1997.
[3] P. Nussbaum, R. Volkel, H.P. Herzig, M. Eisner, S. Haselbeck, Pure Appl. Opt. (UK) 6 (1997) 617–636.
[4] C. Lin, Y. Hsiharng, C. Ching-Kong, J. Micromech. Microeng. 13 (2003) 775–781.
[5] P.E. Dyer, C.D. Walton, Appl. Phys. A: Mater. Sci. Process 79 (2004) 721–727.
[6] J. Li, P.R. Herman, X.M. Wei, K.P. Chen, J. Ihlemann, G. Marowsky, P. Oesterlin, B. Burghardt, Proc. SPIE 4637 (2002) 228–234.
[7] K. Sugioka, Rev. Laser Eng. (Jpn.) 30 (2002) 226–232.
[8] K. Nagashima, M. Hashida, M. Katto, M. Tsukamoto, M. Fujita, Y. Izawa, Trans. Inst. Electr. Eng. Jpn. C (Jpn.) 124 (2004) 388–392.
[9] H. Varel, D. Ashkenasi, A. Rosenfeld, R. Herrmann, F. Noack, E.E.B. Campbell, Appl. Phys. A: Mater. Sci. Process 62 (1996) 293–294.
[10] M.L. Ng, P.R. Herman, A.H. Nejadmalayeri, J. Li, Proc. SPIE 5339 (2004) 127–133.
[11] A. Marcinkevicius, S. Juodkazis, M. Watanabe, M. Miwa, S. Matsuo, H. Misawa, J. Nishii, Opt. Lett. (USA) 26 (2001) 277–279.
[12] J. Wang, H. Niino, A. Yabe, Appl. Phys. A: Mater. Sci. Process 68 (1999) 111–113.
[13] J. Wang, H. Niino, A. Yabe, Appl. Phys. A: Mater. Sci. Process 69 (1999) 271–273.
[14] J. Wang, H. Niino, A. Yabe, Appl. Surf. Sci. 154 (2000) 571–576.
[15] R. Böhme, A. Braun, K. Zimmer, Appl. Surf. Sci. 186 (2002) 276–281.
[16] Y. Yasui, H. Niino, Y. Kawaguchi, A. Yabe, Appl. Surf. Sci. 186 (2002) 552–555.
[17] K. Zimmer, R. Böhme, A. Braun, B. Rauschenbach, F. Bigl, Appl. Phys. A: Mater. Sci. Process 74 (2002) 453–456.
[18] X.M. Ding, T. Sato, Y. Kawaguchi, H. Niino, Jpn. J. Appl. Phys. Part 2: Lett. 42 (2003) L176–L178.
[19] R. Böhme, D. Spemann, K. Zimmer, Thin Solid Films 453–54 (2004) 127–132.
[20] R. Böhme, K. Zimmer, Appl. Surf. Sci. 239 (2004) 109–116.
[21] X.M. Ding, Y. Kawaguchi, T. Sato, A. Narazaki, R. Kurosaki, H. Niino, J. Photochem. Photobiol. A: Chem. 166 (2004) 129–133.
[22] X.M. Ding, Y. Kawaguchi, T. Sato, A. Narazaki, H. Niino, Langmuir 20 (2004) 9769–9774.
[23] G. Kopitkovas, T. Lippert, C. David, S. Canulescu, A. Wokaun, J. Gobrecht, J. Photochem. Photobiol. A: Chem. 166 (2004) 135–140.
[24] R. Böhme, J. Zajadacz, K. Zimmer, B. Rauschenbach, Appl. Phys. A: Mater. Sci. Process 80 (2005) 433–438.
[25] K. Zimmer, R. Böhme, B. Rauschenbach, Appl. Phys. A 86 (2007) 409–414.
[26] X. Ding, Y. Kawaguchi, H. Niino, A. Yabe, Appl. Phys. A 75 (2002) 641–645.
[27] X. Ding, Y. Yasui, Y. Kawaguchi, H. Niino, A. Yabe, Appl. Phys. A 75 (2002) 437–440.
[28] H. Niino, Y. Yasui, X. Ding, A. Narazaki, T. Sato, Y. Kawaguchi, A. Yabe, Proc. SPIE 4977 (2003) 269–280.
[29] Y. Kawaguchi, X. Ding, A. Narazaki, T. Sato, H. Niino, Appl. Phys. A: Mater. Sci. Process 79 (2004) 883–885.
[30] K. Zimmer, R. Böhme, B. Rauschenbach, Appl. Phys. A: Mater. Sci. Process 79 (2004) 1883–1885.
[31] Y. Kawaguchi, X. Ding, A. Narazaki, T. Sato, H. Niino, Appl. Phys. A: Mater. Sci. Process 80 (2005) 275–281.
[32] C. Vass, B. Hopp, T. Smausz, F. Ignacz, Thin Solid Films 453-54 (2004) 121–126.
[33] C. Vass, T. Smausz, B. Hopp, J. Phys. D: Appl. Phys. 37 (2004) 2449–2454.
[34] C. Vass, K. Osvay, B. Hopp, Z. Bor, Appl. Phys. A 87 (2007) 611.
[35] C. Vass, K. Osvay, B. Hopp, Opt. Express 14 (2006) 8354–8359.
[36] H. Niino, X. Ding, R. Kurosaki, A. Narazaki, T. Sato, Y. Kawaguchi, CLEO/Pacific Rim (20032003) 742–1742.
[37] G. Kopitkovas, T. Lippert, J. Venturini, C. David, A. Wokaun, J. Phys.: Conf. Ser. 59 (2007) 526–532.
[38] G. Kopitkovas, T. Lippert, C. David, A. Wokaun, J. Gobrecht, JLMN—J. Laser Micro/Nanoeng. 1 (2006) 23–27.
[39] G. Kopitkovas, T. Lippert, C. David, A. Wokaun, J. Gobrecht, Thin Solid Films 453–54 (2004) 31–35.
[40] G. Kopitkovas, T. Lippert, C. David, R. Sulcas, J. Hobley, A.J. Wokaun, J. Gobrecht, Proc. SPIE 5662 (2004) 515–525.
[41] X. Ding, Y. Kawaguchi, T. Sato, A. Narazaki, H. Niino, Chem. Commun. 17 (2003) 2168–2169.
[42] C. David, J. Wei, T. Lippert, A. Wokaun, Microelectron. Eng. 57–8 (2001) 453–460.
[43] D. Kim, M. Ye, C.P. Grigoropoulos, Appl. Phys. A 67 (1998) 169–181.
[44] H. Niino, Y. Kawaguchi, T. Sato, A. Narazaki, T. Gumpenberger, R. Kurosaki, JLMN—J. Laser Micro/Nanoeng. 1 (2006) 1–6.
[45] F.M. Dickey, S.C. Holswade, Laser Beam Shaping Theroy and Techniques, Marcel Dekker Inc., New York, 2000.
[46] W.W. Duley, UV Lasers: Effects and Applications in Materials Science, Press Syndicate of the University of Cambridge, Cambridge, UK, 1996.